15 January 1996

OPTICS COMMUNICATIONS

ELSEVIER

Optics Communications 123 (1996) 207–214

CW second harmonic generation with elliptical Gaussian beams

A. Steinbach, M. Rauner [1], F.C. Cruz, J.C. Bergquist

Time and Frequency Division, National Institute of Standards and Technology, Boulder, CO 80303, USA

Received 28 April 1995; revised version received 27 September 1995

Abstract

We present a study of the efficiency and optimization of cw second harmonic generation by elliptical Gaussian laser beams. Elliptical focusing slightly improves conversion efficiency and reduces crystal damage risk when heavy walk-off is present. Single-pass measurements of the efficiency for doubling 515-nm radiation in beta-barium borate (BBO) agree with theory. Thermal effects, caused by radiation absorption, limit the doubling efficiency of single-frequency radiation in an external enhancement ring cavity.

1. Introduction

Second harmonic generation (SHG) has become a very useful and widely employed technique to provide monochromatic light sources at wavelengths that are difficult or even inaccessible with conventional lasers. Literature on cw SHG is extensive and explores many possible schemes toward high conversion efficiencies from radiation at the fundamental frequency into radiation at the harmonic. The optimization of cw SHG using spherically focused Gaussian beams was first treated in the most general case by Boyd and Kleinman [1], but SHG using focused Gaussian beams with elliptical cross section offers advantages in some cases. Librechet and Simons [2] show that when critical phase-matching is required, a small increase in doubling efficiency can be expected by using an optimally focused elliptical laser beam rather than an optimally focused circular beam. Asymptotic and exact solutions are found for an ADP crystal with a length of 2 cm and for different values of ellipticity. Comparisons are made between theoretical predictions and experimental values for three choices of ellipticity. Kuizenga [3] treats elliptical focusing for the case of a parametric amplifier and finds that by optimizing the confocal parameters, the threshold for gain can be lowered from that obtained for optimum spherical focusing. This result is valid only when the walk-off parameter B exceeds 1. He also finds that the signal and idler beams remain almost circular while the pump beam grows increasingly elliptical as B increases. Recently, Taira [4,5] has reported high power generation for the second harmonic of a 515-nm argon-ion laser using elliptically focused beams. Motivated by these results, we sought to more rigorously study the generation of second harmonic radiation using cylindrical focusing. We examine conversion efficiencies for a wide range of practical confocal parameters in the critical and noncritical directions and for various values of the walk-off parameter B. For heavy walk-off, we find the the diameter of the light beam in the noncritical direction must remain within a factor 2 of optimum elliptical focusing, otherwise, less harmonic power is generated than for optimum spherical focusing. Our study also

[1] Present address: Institut für Quantenoptik, Universität Hannover, 30167-Hannover, Germany.

SSDI 0030-4018(95)00626-5

reveals no fundamental difference in the far-field mode pattern whether the harmonic radiation is generated by cylindrically or spherically focused light. Measurements of the nonlinear conversion efficiency obatined by single-pass doubling of 515-nm radiation in angle-tuned beta-barium borate (BBO) are presented and compared to theory. We also discuss experimental results obtained by doubling the 515-nm radiation in a Brewster-cut BBO crystal placed in a low-loss external ring cavity using cylindrical mirrors. Although high circulating powers are possible in the absence of harmonic generation, absorption of the UV radiation at 257 nm causes thermal lensing in the crystal that limits the generation of harmonic radiation at higher powers.

2. Theory

In order to calculate the second harmonic power generated by an arbitrary elliptical Gaussian beam passing through a uniaxial nonlinear crystal, we allow fundamental electric fields of the form [6]:

$$E_1(x,y,z) = \frac{E_0 \exp(ik_1 z)}{\sqrt{(1+i\tau_x)}\sqrt{(1+i\tau_y)}} \times \exp\left(\frac{-x^2}{w_{0x}^2(1+i\tau_x)} - \frac{y^2}{w_{0y}^2(1+i\tau_y)}\right), \quad (1)$$

where

$$\tau_i = 2\left(\frac{z-f_i}{b_i}\right), \quad b_i = w_{0i}^2 k_1.$$

Eq. (1) represents an elliptical TEM_{00} Gaussian beam whose focal points (f_x and f_y) and beam waists (w_{0x} and w_{0y}) in the x and y transverse directions are independently adjustable. k_1 is the magnitude of the wave vector inside the crystal. Here we neglect absorption of radiation by the crystal.

In analogy to the heuristic treatment of Boyd and Kleinman, we derive the second harmonic field amplitude in the far field outside the crystal and obtain the power of the second harmonic by integrating over the intensity distribution $(n_2 c/8\pi)|E_2|^2$:

$$P_2 = K P_1^2 l k_1 \cdot \tilde{h}(B, \Delta k, \xi_x, \xi_y), \quad (2)$$

where

$$\tilde{h}(B,\Delta k,\xi_x,\xi_y) = \frac{\sqrt{\xi_x \xi_y}}{l^2} \times \int_0^l \int_0^l \frac{e^{i\Delta k(z'-z)} e^{-4B^2(z'-z)^2\xi_x/l^2}\, dz\, dz'}{\sqrt{1+i\tau_x'}\sqrt{1+i\tau_y'}\sqrt{1-\tau_x}\sqrt{1-\tau_y}}, \quad (3)$$

and

$$K = (128\pi^2\omega_1^2/c^3 n_1^2 n_2)\, d_{\text{eff}}^2$$

$$\xi_i = l/b_i, \quad B = \rho\sqrt{lk_1}/2.$$

τ' differs from τ by replacing z with z'. We use the same coordinate system as in Fig. 1 of Ref. [1] where the optical beam axis is the z direction, the origin is the point where this axis enters the crystal, and the xy-plane is parallel to the crystal faces. The crystal length is l, ρ is the walk-off angle in radians, and n_2 is the extraordinary index of refraction at the doubled frequency. The optic axis of the crystal lies in the xz-plane, and Δk is the wave vector mismatch $(2k_1 - k_2)$. P_1 is the power of the fundamental radiation, d_{eff} is the effective nonlinear coefficient, and n_1 is the ordinary-ray index of refraction.

The second harmonic power is proportional to the function $\tilde{h}(B,\Delta k,\xi_x,\xi_y)$ which, for a given crystal length and amount of input power, contains all variables for optimization. Our numerical calculations show that harmonic power is maximized by adjusting both beam waists to lie at the crystal's midpoint ($f_x = f_y = l/2$). Further, in calculating the harmonic power for a given set of parameters, we use the value of Δk that maximizes the harmonic power. Experimentally Δk can be optimized by temperature or angle-tuning the crystal. Thus, once a particular crystal type is chosen, the waist size in each transverse direction is the only remaining optimizable parameter.

We can solve for second harmonic power as a function of ξ_x, with ξ_y fixed at the value that maximizes $\tilde{h}(B,\Delta k,\xi_x,\xi_y)$ for a given B and Δk. $\tilde{h}$ is plotted in Fig. 1 for a variety of walk-off strengths B and for $\Delta k = \Delta k_m$, the optimum phase-match angle. Comparing these curves to the theoretical predictions for optimized spherical focusing [1] reveals perhaps the most atractive feature of cylindrical focusing: For crystals with heavy walk-off, it is possible to decrease the focusing parameter ξ_x by several orders of magnitude without dropping below the harmonic power that

would be obtained by optimal spherical focusing. It is thus possible to reduce the peak field intensity by several orders of magnitude without lowering conversion efficiency. This reduces the risk of radiation damage to the crystal as well as possible thermal effects.

Optimal cylindrical focusing also improves harmonic conversion efficiency as compared to optimized spherical focusing. For example, for $B = 16$ the optimum focusing parameters are $\xi_x = 0.25$, $\xi_y = 3.3$. This generates 27% more power than that generated for the spherical optimum at $\xi = \xi_x = \xi_y = 1.39$. In all cases where $B \neq 0$, optimal focusing is achieved by a softer focus than the spherical optimum in the transverse direction sensitive to phase matching. When $B = 0$, the cylindrical optimum reduces to the well known spherical focusing optimum given by $\xi = 2.84$. The curves in Fig. 1 are essentially those in Fig. 2 of Ref. [3], which give optimum focusing conditions for parametric gain, and resemble efficiency curves for SHG with spherical focusing in the case that both the harmonic and fundamental power are enhanced in resonant cavities placed around the nonlinear crystal [7–9].

Fig. 2 gives a direct comparison of harmonic power generated by cylindrical and spherical focusing for the case of heavy walk-off. The solid curve gives relative harmonic power versus the spherical focusing parameter $\xi = l/b$ for $B = 16$. The dashed curve represents cylindrical focusing versus ξ_x, also for $B = 16$. ξ_y is fixed at its optimum value of 3.3. Although the increase in efficiency is apparent here (27% for $B = 16$), in practice it may be preferable to decrease the peak field intensity at the crystal surface by decreasing ξ_x, since the loss in second harmonic power can be small. For example, with $B = 16$ it is possible to decrease ξ_x to 0.007 before the harmonic power drops to the maximum possible with spherical focusing. This assumes that ξ_y is fixed at its optimum value of 3.3. The dotted curve in Fig. 2 shows the relative second harmonic power obtained for ξ_y fixed at 1.39, which is the optimal value of ξ for spherical focusing. In this case the somewhat softer focus in the noncritical direction only slightly lowers the nonlinear efficiency from the optimized cylindrical case. But even this nonoptimum curve still rises above the optimum for spherical focusing. Hence, ξ_x can be decreased without sacrificing conversion efficiency, and the lower fundamental intensity reduces the likelihood of crystal damage and the amount of thermal effects.

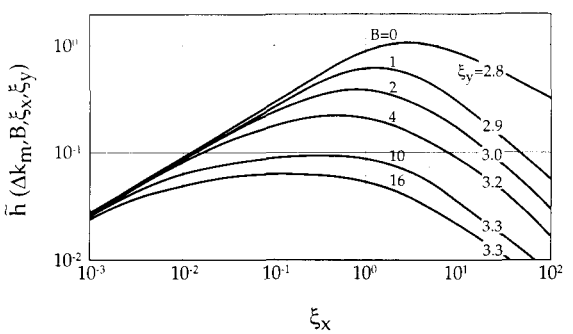

Fig. 1. $\tilde{h}$ maximized with respect to ξ_y for different walk-off parameters B. Δk_m is the optimized value of Δk. For zero walk-off, $B = 0$, the maximum power is the same as in the spherical case; same coordinate system as in Fig. 1 of Ref. [1] where the optical cylindrical focusing technique is only of advantage if energy walk-off occurs. ξ_x approaching zero corresponds to the plane wave limit.

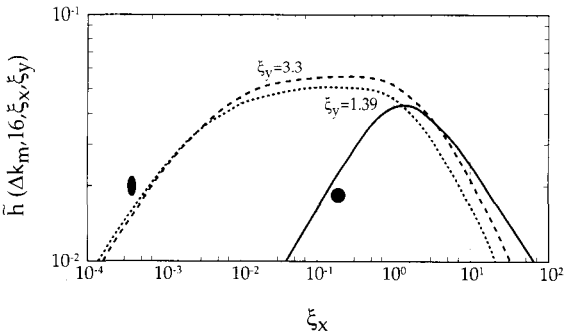

Fig. 2. Cylindrical versus spherical focusing for $B = 16$ and $\Delta k = \Delta k_m$. The focusing parameters which maximize SHG conversion efficiency are $\xi_y = 3.3$ and $\xi_x = 0.25$. For cylindrical focusing ξ_x can be as small as 0.01 before conversion efficiency returns to the maximum value obtained for spherical focusing. The dashed curve represents cylindrical focusing with $\xi_y = 1.39$.

In general, it may not be possible to attain the optimum focusing in either the critical or noncritical direction (for example, in internal or external SHG-setups that use cylindrical elements [4]). For these cases, it would be useful to compare second harmonic generation for non-optimum focusing. In Fig. 3, we show relative harmonic power generation for the case of heavy walk-off ($B = 16$) and various focusing parameters ξ_x and ξ_y. A factor 2 change in the waist size in the noncritical direction away from optimum reduces the maximum harmonic power for cylindrical

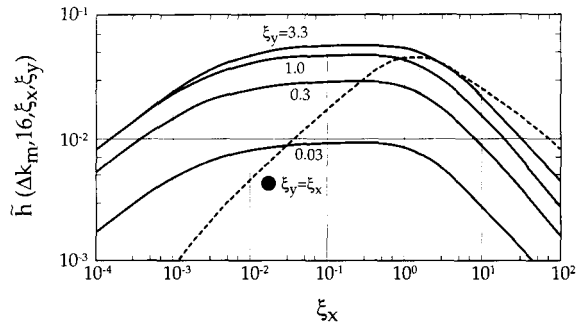

Fig. 3. Dependence of $\tilde{h}$ upon focusing. The conversion efficiency for $B = 16$ is plotted for different ξ_y corresponding to a variation of the waist size in the sagittal (yz) plane. The optimum conversion efficiency can be achieved with $\xi_y = 3.3$. In our experiment, cylindrical mirrors with radius of curvature of 10 cm are used. In this case the values for ξ_y are on the order of 0.1. For comparison, the curve for spherical focusing (•) is also shown.

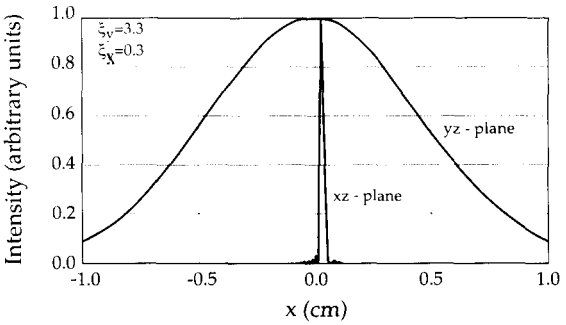

Fig. 4. Second harmonic intensity distribution in the far-field for $B = 12$. The intensity profiles are shown in th x- and y-direction for optimized cylindrical focusing. Whereas the profile in the y-direction is Gaussian, the intensity distributions in the walk-off plane exhibit interference patterns in the wings. An integration over the tangential intensity profile shows that the main lobe contains 96.6% of the total power.

focusing below that obtained for optimum spherical focusing. Clearly it is desirable to remain near optimum focusing in the noncritical direction to realize the full advantages of cylindrical focusing.

The far-field intensity pattern is fundamentally the same for either spherical focusing or cylindrical focusing. Fig. 4 shows the far-field intensity profiles of the harmonic radiation along the x-axis and the y-axis for cylindrical focusing. The interference pattern along the x-axis (the walk-off direction) is due to second harmonic light emitted at different points along the path of the fundamental beam inside the crystal. Since the generated harmonic radiation is emitted under a certain angle relative to the surfaces of equal phase of the fundamental, fringes appear in the intensity distribution. They are also present in the spherical focusing case. However, the amplitude of these fringes is small compared to the amplitude of the main lobe. For both cylindrical and spherical focusing, the main lobe contains over 95% of the total power. In the absence of energy walk-off, the generated radiation would be in phase throughout the crystal and there would be no interference.

The intensity distribution in the walk-off direction is much narrower than the Gaussian intensity distribution in the y-direction. This feature is also common to both methods of focusing. In the spherical case, beam walk-off of the harmonically generated light enlarges the tangential waist of the harmonic compared to the waist in the sagittal plane. In the cylindrical case, both the asymmetric focusing and beam walk-off contribute to the larger waist in the tangential plane. The elliptical cross-section of the second harmonic beam in the far-field is not a serious obstacle. It can be made nearly spherical-Gaussian by means of suitable lenses or mirrors. It has been shown that approximately 89% of the second harmonic radiation can be mode-matched into external resonators that support spherical Gaussian modes [10].

3. Experimental results and discussion

We compared our theoretical predictions to measurements of single-pass SHG conversion efficiencies for various cylindrical focusing geometries. Light from a single-frequency argon-ion laser at 515 nm was doubled to 257 nm in an angle-tuned, Brewster-cut BBO crystal. Combinations of cylindrical and spherical lenses and mirrors were used to create the various TEM_{00} elliptical Gaussian beams. The BBO crystal length is 6.5 mm and the walk-off angle ρ is 0.085 rad; hence, $B = 15.6$. In Fig. 5, the solid line represents the theoretical SHG conversion efficiency for $B = 15.6$ as a function of ξ_x. ξ_y is fixed at 2.4, which corresponds to the 15 μm value of w_{0y} that was used for all our experimental data points (this value is near the optimum value for cylindrical focusing that gives $\xi_y = 3.3$ and $w_{0y} \simeq 13$ μm). The single-pass conversion efficiency η is given by $P_2 = \eta P_1^2$, where

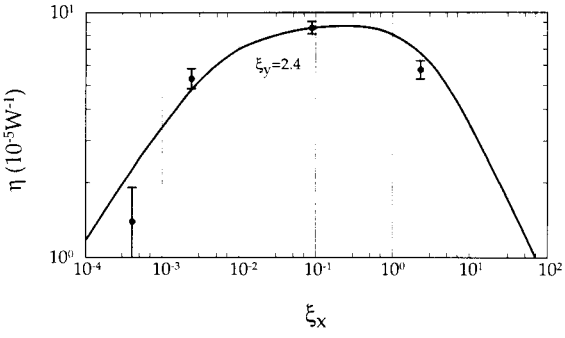

Fig. 5. Comparison of theoretically predicted values and experimental data for the single-pass conversion efficiency. In the experiment, the waist size and position in the (noncritical) yz-plane is kept fixed at 11.5 μm, while the waist size in the walk-off plane is varied by means of different lens combinations. The theoretical curve is calibrated by deriving d_{eff} for our BBO crystal from a single-pass conversion efficiency measurement under optimum spherical focusing conditions.

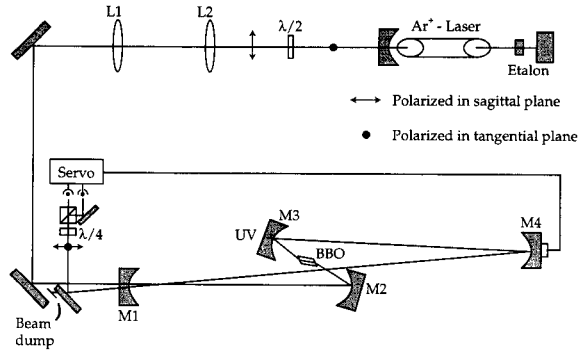

Fig. 6. The experimental setup for generating high-power 257-nm radiation. The single-frequency green light ($\lambda \simeq 515$ nm) of an argon-ion laser is doubled with a Brewster cut and polished BBO crystal placed in an external ring resonator. M1 (input coupler) and M4 are spherical mirrors with a radius of curvature of 30 cm. In order to produce a Gaussian mode with an elliptical cross section, M2 and M3 are cylindrical mirrors with a radius of curvature of 10 cm in the plane of the drawing. M3 is highly reflecting for 515 nm and highly transmitting for 257 nm.

P_2 is the output harmonic power. The theoretical peak height depends on the value of d_{eff} used. The value of d_{eff} for our crystal was derived from a single-pass measurement under optimum spherical focusing conditions ($w_0 \simeq 20$ μm). We measured the efficiency to be 7.0×10^{-5} W^{-1} which gives $d_{\text{eff}} \simeq 0.32$ pm/V (subsequently we obtained a second BBO crystal from another vendor and measured its single pass efficiency to give $d_{\text{eff}} \simeq 0.4$ pm/V). In Fig. 5 the data points represent the measurements of single-pass efficiency as a function of ξ_x. The agreement between the theoretical curve (B = 15.6, ξ_x=2.4) and the experimentally obtained values is good. The error bars account for statistical error.

In applications that need high second harmonic power, cylindrical focusing can be achieved easily with optical cavities that boost the amount of fundamental power incident on the crystal. High power, cw 257-nm generation, obtained by doubling the frequency of an argon-ion laser in an intracavity setup, has been demonstrated [4] with cylindrical lenses as focusing elements. In Fig. 6 we show a simple frequency doubling scheme where the crystal is placed between two cylindrical mirrors in an external ring resonator. This configuration avoids the additional losses introduced by intracavity lenses and the complications and expense of low-loss AR coatings for both the fundamental and the harmonic. Mirrors M2, M3 and M4 have a high reflectivity ($R \geq 0.998$) at the 515-nm wavelength of the argon-ion laser and the transmission of the input coupler M1 is about 1.8%. The cylindrical mirror M3 transmits 94% of the generated UV at 257 nm. Two spherical lenses, L1 and L2, constitute a telescope to establish mode-matching into the cavity. The cavity is locked to resonance by means of the Hänsch-Couillaud locking scheme [11].

M1 and M4 are spherical mirrors with matching radii of curvature of 30 cm. M2 and M3 are cylindrical mirrors with a radius of curvature of 10 cm. The eigenmode of the resonator is spherical-Gaussian, except in the region between the two cylindrical mirrors where the cross section of the beam is elliptical. Since M2 and M3 act as flat mirrors for the tangential component of the beam, the cavity is free of astigmatism other than the small amount due to the off-axis incidence on mirrors M1 and M4. The angles of incidence on all mirrors can be made small to minimize most higher-order aberrations. Maximum conversion efficiency is obtained when both the tangential and the sagittal focus are centered inside the crystal. Therefore the ideal alignment is symmetric about the crystal.

The lowest order TEM_{00} eigenmode of the resonator exhibits comparatively soft focii ($w_{0x} \simeq 200$ μm) at the middle of the crystal as well as halfway between M4 and M1. In the sagittal plane the cylindrical mirrors focus the beam more tightly ($w_{0y} \simeq 50$ μm).

Faster cylindrical mirrors are needed to come closer to the optimum focusing condition where $w_{0x} \simeq 46$ μm, $w_{0y} \simeq 13$ μm for $B = 15.6$ and $l = 6.5Z$ mm. A cavity using cylindrical mirrors with a radius of curvature of about 3 cm in combination with a pair of spherical mirrors with a radius of curvature of 30 to 50 cm can establish near optimum focusing conditions. Theoretically, an improvement in the doubling efficiency of about 2.5 can be expected as compared to our current setup.

For Brewster cut, highly transparent crystals, linear intracavity losses are usually dominated by light scattering from the crystal surfaces due to imperfect polishing and by a small transmission of the fundamental radiation through the highly reflecting mirrors. We determined the round-trip linear loss term of the cavity to be about 0.7% (for the second, more efficient BBO crystal) from the mode-matched power enhancement factor of about 115. For this measurement, the angle of the BBO crystal is adjusted so that no harmonic radiation is generated. Since the transmission of the input coupler is 1.8%, not all of the fundamental power is coupled into the cavity. Ideal coupling (no power reflected from the input coupler) is obtained when the transmission of the input coupler equals the round-trip intracavity loss term [12]. However, when the BBO crystal is again angle tuned so that harmonic radiation is generated, the impedance match improves as the fundamental power is increased, because the nonlinear loss term increases as a greater fraction of the circulating fundamental power is converted to UV light [13,14]. The losses due only to the mirrors were determined to be 0.35% by measuring a power enhacement factor of about 156 for the cavity without the crystal. Therefore the linear losses due solely to the crystal are also about 0.35%.

We measure the fundamental power enhancement in two ways; either by sweeping the cavity through resonance or by locking the cavity to resonance. In both cases, the power leaking through one of the highly reflecting cavity mirrors is compared to the power transmitted by the same mirror with the input coupler to the cavity removed. We expect both methods to give identical results unless there are thermal problems which degrade the power enhancement when the cavity is locked to resonance [14]. For input powers less than 250 mW, the power enhancement factor in the fundamental mode, measured by either method, is about 110 ($\sim$ 5% of the input power was coupled into higher-order modes). As the input power is increased, the enhancement factor (again measured by either method) begins to decline as the loss term due to nonlinear conversion of fundamental radiation into second harmonic light increases. However, for input powers exceeding approximately 1 W (85-90 W intracavity), the power amplification factors measured by the swept method and the locked method begin to diverge. When locked to resonance, the circulating power is less than that measured for the swept case, presumably due to radiation absorption that causes thermal lensing in the crystal [14]. The divergence increases as the input power is raised (2.1 W is the single-mode power limit of our present laser). If the crystal is angle detuned so that harmonic generation does not occur, than the power enhancement factor remains about 110 for all input powers whether measured when locked to resonance or swept . Interestingly, the conversion efficiency η also drops for higher powers as the thermal effects become more prominent. η remains near 4.5×10^{-5} W^{-1} for our cavity focusing conditions and for power inputs up to 1 W, then begins to decrease (remember that η depends on the focusing parameters which change as the thermal lensing increases). At 2 W into the cavity the build-up on resonance is only 63. The amount of absorption and radiative heating seems to vary widely from crystal to crystal, even for BBO [15,16]. The cavity power enhancement for our poorer crystal drops from about 90 to nearly 40 at 2 W input power and we are unable to stably lock the cavity to resonance at 2 W input power. For the better BBO crystal, an input power of 380 mW generates 64 mW of UV power; at a fundamental input power of 1.9 W, the cavity can still be stably locked to resonance and approximately 500 mW of harmonic power is produced. Although we made no long term measurements of the stability of the harmonic power, the 500 mW was reproducible day-to-day and stable for 30 minute periods. These and other values for different input powers are plotted in Fig. 7a. The values for the UV power have been corrected for the 94% mirror transmission and the 20% Fresnel loss at the exit face of the Brewster cut crystal. The solid line in Fig. 7a represents the theoretical expectation for the harmonic output obtained from :

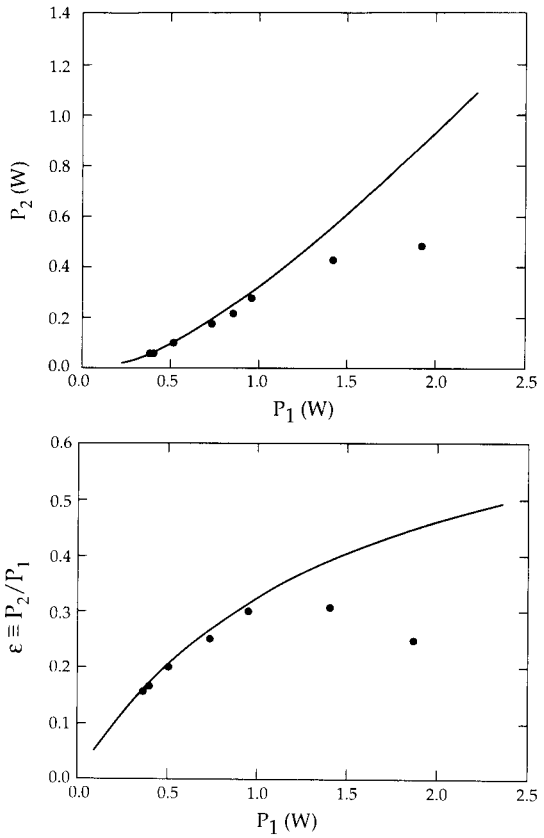

Fig. 7. (a) Second harmonic power P_2 as a function of fundamental input power P_1 at $\lambda = 515$ nm. (b) Overall conversion efficiency $\epsilon \equiv P_2/P_1$ as a function of input power P_1 . The solid line curves are derived from Eq. (4) using the measured values $\eta = 4.2 \times 10^{-5}$ W^{-1}, $L = 0.7\%$ and $T = 1.8\%$.

$$\sqrt{\varepsilon} = \frac{4T\sqrt{\eta P_1}}{[2 - \sqrt{1-T}(2 - L - \sqrt{\varepsilon\eta P_1})]^2}, \qquad (4)$$

where $\varepsilon \equiv P_2/P_1$ denotes the overall conversion efficiency, T the transmission of the input coupler, and L the cavity round-trip linear loss term [13,14]. Eq. (4) includes the nonlinear loss factor in the last term in the denominator. The deviation of the experimental results from the theoretical prediction above 1 W of input power reveals the thermal effects due to absorption of harmonic radiation. In Fig. 7b, the theoretical (solid line) and experimental values of ε are plotted which also clearly show the deviation caused by thermal effects in the BBO crystal. Our best values for overall conversion efficiency slightly exceed 30%. While better conversion efficiences can be expected for optimum focusing and better impedance matching at low input powers, the thermal effects caused by radiation absorption may worsen for the tighter focusing and severely limit η at higher powers [2].

4. Conclusion

In conclusion, we have calculated efficiency curves for harmonic generation for the general case of cylindrical focusing for a wide range of confocal parameters and for practical values of beam walk-off. We have shown that, for angle-tuned harmonic generation, elliptical focusing can produce the same or slightly more harmonic power than spherical focusing for the same fundamental power. Also, since the intensity can be lower for elliptical focusing, the risk of radiation damage to the crystal can, in principle, be reduced. Measurements of single-pass efficiency are in agreement with these calculations. We have shown the the far-field intensity distribution for the harmonic radiation is the same whether the fundamental beam is cylindrically or spherically focused. We have also built a simple, low-loss external ring cavity using cylindrical mirrors and an intracavity, Brewster-cut BBO crystal. The cavity had a mode-matched power enhancement factor of about 110, for light at 515-nm. Thermal lensing in our crystal limited the overall conversion efficiency to about 30%. Even though we achieved slightly higher conversion efficiencies in BBO with cylindrical focusing, the thermal lensing effects limited the useful fundamental power in the external cavity to a level where a simpler spherical cavity would offer no risk of crystal damage. From our results, we conclude that the small increase in second harmonic power due to elliptical focusing probably does not warrant the expense and complication of cylindrical mirrors or lenses.

[2] We note that Kubota et al. [16] were able to achieve a stable output power of about 800 mW at 266 nm by doubling 532 nm radiation in BBO in an external ring cavity. This would either imply a better BBO crystal with extremely low absorption in the ultraviolet, or that the absorption at 266 nm is lower than at 257 nm.

Acknowledgements

We thank H. Patrick and M. Young for careful reading of the manuscript. F.C. Cruz is pleased to acknowledge the financial support of CAPES (Brazil).

References

[1] G.D. Boyd, D.A. Kleinman, J. Appl. Phys. 39 (1968) 3597.
[2] F.M. Librecht and J.A. Simons, IEEE J. Quantum Electron. 11 (1975) 850.
[3] D.J. Kuizenga, Appl. Phys. Lett. 21 (1972) 570.
[4] Y. Taira, Jpn. J. Appl. Phys. 31 (1992) L682.
[5] Y. Taira, CLEO'93 proceedings, pp. 634–637.
[6] A. Yariv, Quantum Electronics (Holt, Rinehart and Winston, New York, 1976) p. 51.
[7] C. Zimmermann, R. Kallenbach, T.W. Hänsch and J. Sandberg, Optics Comm. 71 (1989) 229.
[8] Z.Y. Ou and H.J. Kimble, Optics Lett. 13 (1993) 1053.
[9] K. Fiedler,S. Schiller, R. Paschotta, P. Kürz and J. Mlynek, Optics Lett. 18 (1993) 1786.
[10] M. Boshier, Ph.D. Thesis, University of Oxford (United Kingdom), 1988; available from UMI in association with the British Library.
[11] T.W. Hänsch and B. Couillaud, Optics Comm. 35 (1980) 441.
[12] J.C. Bergquist, H. Hemati and W.M. Itano, Optics Comm. 43 (1982) 437.
[13] W.J. Kolowsky, C.D. Nabors and R.L. Byer, IEEE J. Quantum Electron. 24 (1988) 913.
[14] E.S. Polzik and H.J. Kimble, Optics Lett. 16 (1991) 1400.
[15] Coherent, private communication;
Y. Taira, private communication.
[16] Kubota et al., Optics Lett. 19 (1994) 189.